

Middle Pleistocene to Holocene geochronology of the River Aguas terrace sequence (Iberian Peninsula): Fluvial response to Mediterranean environmental change

Lothar Schulte^{a,*}, Ramon Julià^b, Francesc Burjachs^c, Alexandra Hilgers^d

^a Department of Physical and Regional Geography and Laboratory of Landscape Research, University of Barcelona, C/Montalegre 6, E-08001 Barcelona, Spain

^b Institute of Earth Science “Jaume Almera”, CSIC, C/Lluís Sole i Sabaris s/n., E-08028 Barcelona, Spain

^c ICREA at the Department of Prehistory, University Rovira i Virgili, Plaça Imperial Tàrraco 1, E-43005 Tarragona, Spain

^d Department of Geography, University of Cologne, Albertus-Magnus-Platz, D-50923 Köln, Germany

Received 7 February 2006; received in revised form 28 July 2006; accepted 27 March 2007

Available online 17 May 2007

Abstract

Our results from the River Aguas basin suggest that fluvial archives, travertine and slope deposits provide sensitive resolution records of environmental changes during the last 170 kyr. From the chronostratigraphic data sets we have established a model of middle and late Pleistocene river response for littoral basins on the southern Iberian Peninsula.

U/Th and OSL dating indicate the major periods of travertine formation of the Alfaix travertine platform, which range from 169 to 26 kyr. At least four incision events interrupted this aggradation period: between 167 and 148 kyr, between 148 and 110 kyr, around 95 kyr and at 71 kyr. Aggradation ceased after 26 kyr and incision occurred during OIS 2. Subsequently, the terraces T4a and T4b were deposited. OSL dating of the T4a channel deposit provides maximum ages of 28, 20 and 18 kyr. However, short climatic events, such as the Younger Dryas, produced two more river incision episodes during OIS 2.

Nonetheless, for river systems influenced by tectonics, climate and sea-level changes it is difficult to assess the weight of each controlling factor. Regarding the three mechanisms of Pleistocene river dynamics in middle-size catchment areas of the littoral region of southeastern Spain, our results support the hypothesis that large scale tectonics triggered the general downcutting trend, whereas the main aggradation and incision phases occurred during periods of major sea-level changes. Over short-time scales the influence of climate variability, as documented by pollen records, plays a decisive role. Thus, the river responses to the three cyclic mechanisms operate at different time scales although synergetic processes should be considered with respect to the magnitude of abrupt incision/aggradation events.

© 2007 Elsevier B.V. All rights reserved.

Keywords: Fluvial terraces; Sea-level changes; Pollen analysis; Geochronology; Late Pleistocene; Iberian Peninsula

1. Introduction

The chronology of fluvial erosion and deposition has the potential to identify tectonic, climate and human-induced environmental changes (Gregory et al., 2006).

* Corresponding author.

E-mail address: schulte@ub.edu (L. Schulte).

Vandenberghe (2003), however, has suggested that the development of river systems can be considered in terms of specific climatic parameters: climate-derived factors, partially climate-dependant factors, and non-climatic factors.

The arid and semi-arid landscapes of southeast Spain developed on the tectonically active Betic system have attracted much attention from geomorphologists. Since the pioneering work of Völk (1967, 1979) on the Neogene geology and Quaternary geomorphic evolution of the Vera basin, a significant number of Quaternary river terraces chronosequences have been established in the Cenozoic basins of the Internal Zone of the Betic Cordillera: Wenzens (1992) and Stokes and Mather (2003) studied the Almanzora catchment, Mather et al. (1991), Harvey et al. (1995), and Candy et al. (2005) the upper and middle reaches of the River Aguas and Schulte (1998, 2002a) the middle and lower reaches of the Aguas and Antas rivers. Although Quaternary tectonics, river capture, climate and sea-level control were repeatedly cited, how these variables influenced river dynamics in the Aguas valley remains unclear.

The aim of this paper is to provide evidence about the origin of the fluvial terraces of the middle and lower River Aguas in southeastern Spain. Therefore, we focused on two questions. Firstly, do fluvial archives in southeast Spain provide sensitive records of climate changes during the last 170 thousand years? And secondly, how do climate, sea-level changes and tectonics affect fluvial dynamics?

2. Regional setting

The 539 km² catchment of the River Aguas covers the eastern Sorbas basin and the southern Vera basin located between 37°20'N and 37°2'N and between 2°9'W and 1°48'W (Fig. 1). It is located on the tectonically active eastern margin of the Betic Ranges (López Casado et al., 2001; Negro et al., 2002; Booth-Rea et al., 2004; Gràcia et al., 2006). The Sorbas and Vera basins developed since the Middle Miocene as pull-apart basins connected to the Alborán basin (Braga et al., 2003). The Miocene deposits consist of interbedded marine marl, reef-limestone, calcareous sandstone, siltstone, gypsum and conglomerate. The late Neogene uplift of the Betic Cordillera led to the subsequent shift from marine to continental sedimentation environments from the inner to the outer basins of the Betic Internal Zone (Fig. 1). The youngest marine deposits date to the end of the Messinian in both the Huerca-Overa and Sorbas basins (Roep et al., 1998). In the Vera basin marine regression and subsequent progradation of delta

conglomerates of the Espíritu Santo Formation occurred during the late Pliocene. At the end of the Pliocene the basin was tectonically uplifted, ending the marine influence from the central part of the Vera basin (Montenat et al., 1990). During this phase, pediments (P1 of Schulte, 2002a) were cut and thick alluvial fans (S1 and S2; Schulte, 2002a), correlating with the Raña Formation of central Spain (Wenzens, 1992), were deposited along the depression margins. Since the Early Pleistocene the Vera basin was drained by three river systems: The Almanzora river in the north, the Antas river in the centre, and the proto-River Aguas in the south.

During the Pleistocene the Aguas and the Jauto rivers shaped basins situated at altitudes between 0 and 400 m a.s.l., and generated up to 15 geomorphic levels consisting of pediments, alluvial fans, glaciais, fluvial, and travertine terraces (Fig. 2; Schulte, 2002a). The readily eroded Neogene marls of the basin fill increase edaphic aridity and constitute an important source of carbonates to the fluvial terraces. These terraces are formed by cobbles, gravels and sands of metamorphic rocks (schist, quartzite and gneiss) and sedimentary rocks (limestone, marl, sandstone, conglomerates, and dolostone).

The dominant long-term incision of the fluvial network was triggered by the tectonic uplift of the basin. However, compressional tectonics led to the west-east oriented synforms and antiforms in the eastern Sorbas basin (Booth-Rea et al., 2004; Fig. 1) and caused local subsidence. The neotectonic activity can be observed by the deformation of the middle and late Pleistocene fluvial, travertine and marine deposits.

Regional palaeoclimatic data covering the Middle Pleistocene to Holocene are abundant in the southeastern Iberian Peninsula. Marine cores from the Alborán Sea provide clear evidence of sea surface temperature changes (Grafenstein et al., 1999; Moreno et al., 2002) related to solar forcing and abrupt vegetation changes related to Heinrich events (Kageyama et al., 2005). In addition, continental pollen records indicate abrupt climate change during Late Pleistocene and Holocene sequences (Florschütz et al., 1971; Pons and Reille, 1988; Pantaleón-Cano et al., 1996; Burjachs et al., 1997). These climate (and vegetation) changes affected fluvial dynamics and soil processes (Harvey et al., 1995; Schulte and Julià, 2001; Günster et al., 2001; Schulte, 2002b, 2003; Thorndycraft and Benito, 2006).

Longitudinal profiles reconstructed by Schulte (2002a) suggest that tectonic activity, the lithology of the Neogene bedrock and river capture are together responsible for several knick-points developed along the

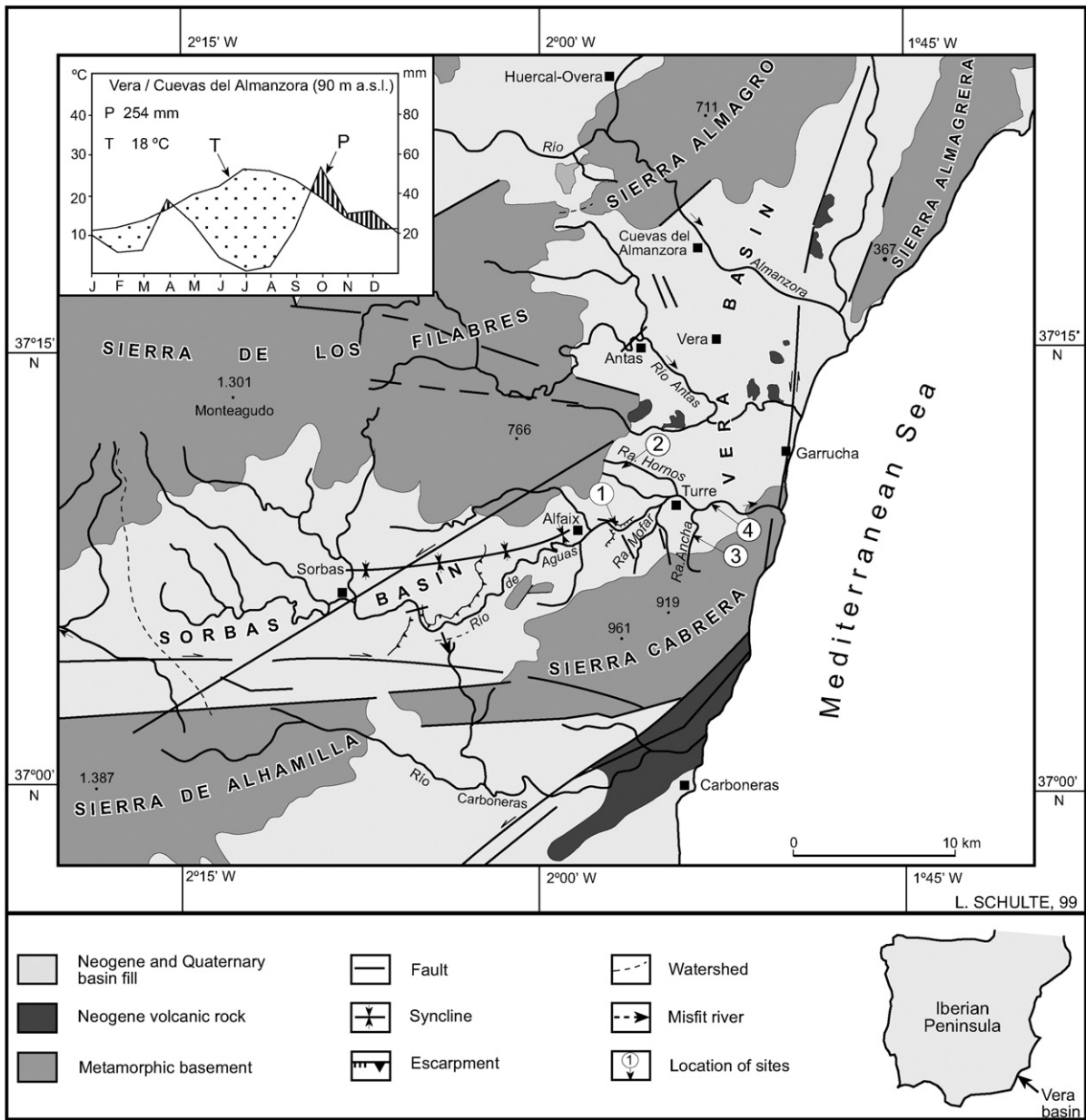


Fig. 1. Geographical location of the study sites. 1=Alfaix travertine sequence. 2=Fluvial terrace T4a at Rambla de los Hornos. 3=Rambla Ancha site. 4=LGM/Holocene terrace intersection at 4 km to the coastline.

River Aguas bed at 11 km, 18 km, 24 km and 26 km from the coast. This paper focuses on two particular sections. The first, the Alfaix travertine, is located upstream of the lowest knick-point of the River Aguas (Fig. 2) in the transition zone between the eastern corridor of the Sorbas basin and the western margin of the Vera basin. The Neogene deposits of the Alfaix area consist of resistant calarenites (where knick-point occurs) and erodible marls, tectonically affected by faults and a synclinal fold.

The T3 and T4 terraces are not preserved 3 to 4 km downstream of the Alfaix knick-point because of the predominance of erosion processes at the Molino de la Cueva gorge. In the lower reach of the River Aguas the T3 and the T4 terrace surfaces are located at 12 and 8 m above present riverbed, whereas the bottoms of the fluvial deposits of these terraces are not exposed due to terrace intersection.

The second section corresponds to the +8 m terrace of a northern tributary of the River Aguas, the Rambla

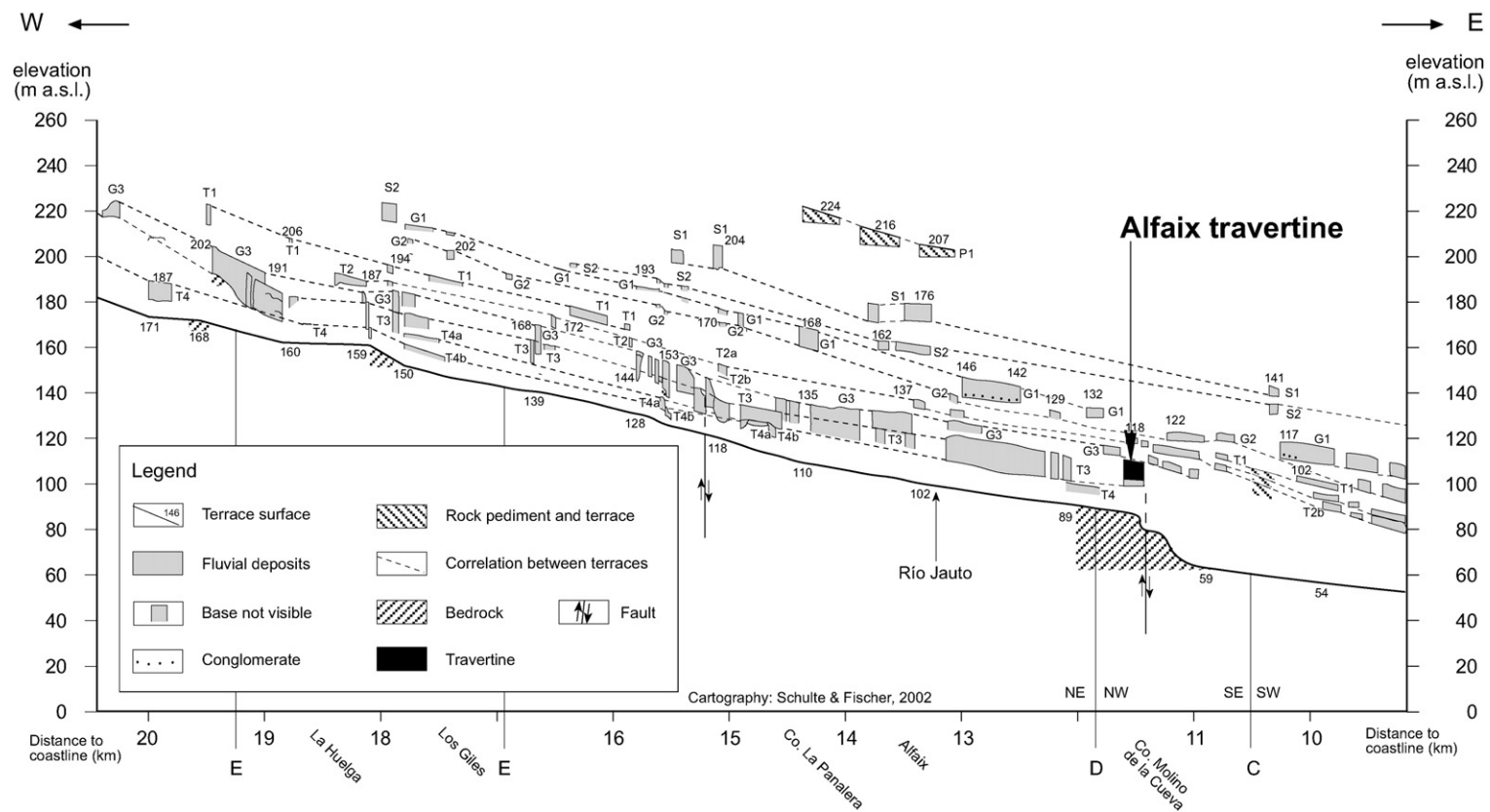


Fig. 2. Longitudinal profiles of the fluvial terraces of the middle reach of the River Aguas. The terrace profiles of lower and the upper reach of the River Aguas are published in Schulte (2002a).

de los Hornos. We chose this location because the lower terraces of the River Aguas are not well preserved owing to intensive agricultural land-use and irrigation systems.

According to *Rivas Martínez (1987)* the Vera basin is dominated by plant associations formed by typical elements of the Mediterranean semi-arid climate. The main associations correspond to *Mayteno–Periplocetum angustifoliae* and *Chamaerops–Rhamnetum lycioides*. However, human pressures (agriculture, grazing and mining) have substantially disturbed this natural vegetation.

The semi-desert vegetation cover offers little protection against erosion resulting from thunderstorms (mainly in spring and autumn). Today the total annual precipitation is approximately 250 mm yr⁻¹ and the mean annual temperature is 18 °C (*ICONA, 1991*). Although at present soil formation under these conditions is very limited, during former humid climates paleosols, such as xeralfs, developed on the stable land surfaces. An extensive soil chronosequence was established by *Schulte and Julià (2001)* for the lower Aguas reach.

3. Materials and methods

The depositional and incisional history of the River Aguas was reconstructed using methods from disciplines of geomorphology, sedimentology, soil science, palynology and geochronology. In this paper we focus on two key sections. The first corresponds to the Pleistocene Alfaix travertines and the +12 m river terrace T3 (site code Ag-620), whereas the second refers to the +8 m river terrace T4 (site code Ag-344).

The chronology of the river terrace sequence was determined from geomorphological and sedimentological criteria, U/Th, optically stimulated luminescence (OSL), ¹⁴C, ²¹⁰Pb radiometric dating as well as from artefacts (*Schulte, 1998, 2002a*).

3.1. Geomorphology

Pleistocene and Holocene fluvial terrace flights, over a reach of more than 30 km between the Sorbas village and the River Aguas mouth, were mapped in detail (scale 1:10,000) and checked with aerial photographs (scale 1:18,000). Based on published maps (1:10,000) spot height and altimeter readings were calibrated in the field. The height of terrace surfaces is accurate to ±1 m. Such precision is required to draw accurate longitudinal profiles (horizontal scale of 1:10,000 and vertical scale of 1:1000) that will permit correlation between the hundreds of small-size river terrace remnants affected

by faulting and tilting. The morphostratigraphy of the 15 terrace levels was defined by height above river bed, thickness and sedimentology of the terrace deposits and palaeosol development (*Fig. 2*). The morphological map of the Quaternary fluvial deposits of the middle and lower reach of the River Aguas was published by *Schulte (2002a)* at a 1:25,000 scale.

3.2. Sedimentological and palynological studies

Sedimentological descriptions and sampling were carried out in fluvial, slope, and travertine deposits as well as in soils. Samples of the south-western vertical escarpment of the Alfaix travertines were obtained by abseiling, explaining why U/Th-data sets had to be obtained from different sections.

Samples for pollen analysis were taken at the Alfaix key section (sample codes Ag-481, Ag-620, Ag-699) at irregular intervals and preferably from travertine samples used for U/Th dating, whereas alluvial sediments of terrace T4 were sampled at 10 cm intervals. The pollen samples were treated using the *Goehry and de Beaulieu (1979)* technique, which was slightly modified according to *Burjachs et al. (2003)*. To calculate AP/NAP percentages, we excluded Asteraceae, Cyperaceae and Cerealia-type pollen taxa from the basic sum. For the calculation of the pollen concentration (PC) we have used the volumetric method (*Loublier, 1978*).

In the case of key section Ag-344 of the fluvial terrace T4 we took 15 samples for laboratory analysis. The determination of organic carbon was performed by combustion–reduction–gas chromatography. The pedological findings of the key sections were integrated in the regional Quaternary soil chronosequence proposed by *Schulte and Julià (2001)*.

3.3. Travertine sampling and U-series disequilibrium dating procedures

Travertines are carbonate deposits appropriate for U-series disequilibrium dating procedures. In Spain these sediments have been largely used for dating Late Pleistocene and Early Holocene archaeological and perched travertine sequences (*Bischoff et al., 1988; Julià and Bischoff, 1991*). *Bischoff et al. (1994)* demonstrated that U-series dates of the Abric Romani (NE-Iberian Peninsula) travertine deposits fit well with the AMS dates on charcoal particles. U-series disequilibrium dates have been used to provide fluvial chronostratigraphical frameworks for Iberian river systems (*Benito et al., 1998; Diaz-Hernández and Julià, 2006; Luque and Julià, 2007*).

Sixteen samples were taken in the travertine deposits (Fig. 3) to apply the Uranium series disequilibrium method (Ivanovich and Harmon, 1982) on the most dense calcite deposits such as oncolithes or encrusted vegetal debris. Sampling was carried out in the internal part of each travertine bed, in order to avoid surface contamination and any recrystallized portions. Uranium and Thorium radioisotopes were isolated and purified from each sample by conventional techniques of total sample dissolution by acids and ion-exchange chromatography, and electroplated in silver. The isotopic composition was determined by alpha spectroscopy, following the procedures described in Bischoff and Fitzpatrick (1991).

Nominal dates are calculated from the daughter/parent $^{230}\text{Th}/^{234}\text{U}$, and assume that all the contained ^{230}Th was formed by in situ decay from contained ^{234}U . Nevertheless, the isotopic results show that a slight contamination of ^{232}Th existed during the travertine formation probably associated with siliciclastic contribution into travertine deposits.

Nominal dates, in general, are significantly older according to the degree of thorium contamination. Julià and Bischoff (1991) found that the detrital contamination begins to significantly affect the nominal ages when $^{230}\text{Th}/^{232}\text{Th}$ ratio is less than about 17. Samples that are contaminated show older ages.

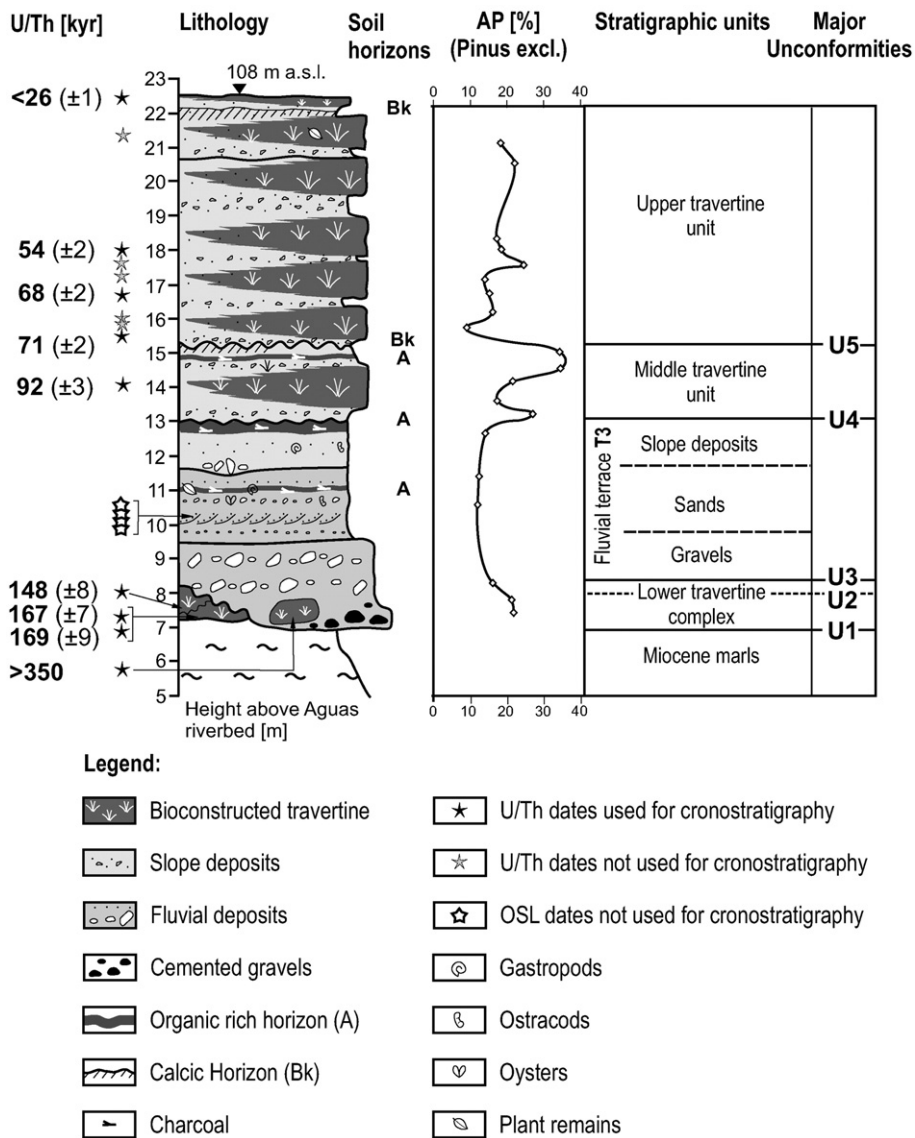


Fig. 3. Lithology and chronology of the Alfaix travertine key section. Geographical location in Fig. 1.

3.4. Luminescence dating

Luminescence dating was carried out at the luminescence dating laboratory of the Department of Geography, University of Cologne. The OSL measurements were carried out on the quartz or potassium-rich feldspar fraction in the grain size range of 0.1–0.2 mm. In general, the single-aliquot regenerative-dose protocols (SAR) described by Murray and Wintle (2000) and Wallinga et al. (2000) were used for sand-sized quartz and K-rich feldspar extracts, respectively. Several subsamples, or aliquots, were measured per sample to obtain equivalent dose (D_e) values (see Table 2) and estimates of the amount of radiation dose accumulated within the crystal lattice of a mineral grain since it was shielded from sunlight. To calculate the annual dose (D_0) derived from the decay of lithogenic radionuclides in the sediment the concentration of uranium, thorium, and potassium was determined by neutron activation analysis (NAA, Becquerel Laboratories, Sydney, Australia; Table 2). Attenuation of ionising radiation is more effective in sediments with water-filled interstices. Therefore changes in the sediment moisture content since deposition affect the dose rate calculation. In order to allow for this, a water content variation of 2 to 16% was finally assumed rather than using the ‘as found’ moisture content ranging from 1.3 to 2.4 wt.%.

4. Results

4.1. Geochronology

The geochronological framework of the River Aguas fluvial deposits is based on 16 U/Th dates, 7 OSL dates and 7 AMS (5 dates published in Schulte, 2002b and 2 dates in this paper).

4.1.1. U-series dating

Table 1 shows the results of the radiometric data obtained by alpha spectroscopy. Only eight samples show low contamination with ^{232}Th ($^{230}\text{Th}/^{232}\text{Th} > 17$) and can be used as chronological data (Julià and Bischoff, 1991): one from a travertine tilted block outcropping over the Neogene marls (>350 ky), three from the lower travertine platform (covering an elapsed period between 169 ± 9 kyr and 148 ± 8 kyr), three more from the middle travertine platform (between 92 ± 4 kyr and 69 ± 2 kyr), and one at 4 m below the travertine platform surface (55 ± 2 kyr). Another sample with relatively low detrital contamination indicated by a $^{230}\text{Th}/^{232}\text{Th}$ ratio of 10 and its chronological data can be used as an approximate age. This sample is from the

middle travertine platform, with a nominal date of 69 ± 2 kyr. The ^{232}Th content of the other seven samples vary between 0.42 ppm and 0.21 ppm (Table 1), their nominal dates, calculated directly from the daughter/parent ratio, must therefore be rejected assuming that the measurement of the ^{230}Th daughter derived from the contained ^{234}U .

4.1.2. Luminescence dating

The luminescence ages obtained for the quartz and the feldspar samples taken from T4a sediments overestimate the expected depositional ages derived from the U/Th, AMS and artefact-dated fluvial chronostratigraphy of the River Aguas (see discussion in Section 5.1). As the measurements yielded evidence for incomplete resetting of the luminescence signals prior to deposition for all samples and for both mineral fractions, all luminescence ages obtained for T4 samples should be interpreted as maximum ages only. Poor bleaching, not unlikely for fluvial deposits (Wallinga, 2001), was identified on the basis of a comparison of the data spread among the individual D_e estimates of the natural samples (expressed as relative standard deviation, RSD) with that obtained for the ‘dose recovery test’ (DRT) samples. While the dose distributions of the artificially completely bleached and subsequently irradiated DRT samples yielded RSD values of 12% for quartz and for several tests using feldspar only of 1.5–6.8%, the natural dose distributions showed significantly higher values (Table 2). Inhomogeneities in the beta radiation field, microdosimetry effects (Wallinga, 2001), which are also known to cause a substantial spread in equivalent doses, are regarded as less likely to be a problem for these samples. This is because, with a large percentage of their dose rate coming from ^{40}K within the grains, K-feldspars ought to show a significantly lower scatter compared to quartz, however that was not observed here. The difference in quartz and K-feldspar ages may be ascribed to an even higher residual signal in feldspar extracts from the same sample, as bleaching is not as rapid and effective as in quartz (Godfrey-Smith et al., 1988). Thus, the systematically younger quartz ages are assumed to better represent the true depositional ages. The best approximation to the true ages is presumably achieved by processing the data sets as described by Fuchs and Lang (2001) resulting in age values of about 20, 18, and 28 ka for samples Ag-344.23, Ag-344.24, and Ag-344.25, respectively.

Based on the data spread observed in the feldspar measurements of the T3 deposits, it can be assumed that all but sample Ag-620.21, and perhaps sample Ag-620.24, are also affected by incomplete bleaching.

Table 1
U-series disequilibrium dating of the Alfaix travertine sequence

Sample ID*	Lab-ref	m over riverbed*	U [ppm]	Th [ppm]	$^{234}\text{U}/^{238}\text{U}$	$^{230}\text{Th}/^{234}\text{U}$	$^{230}\text{Th}/^{232}\text{Th}$	Nominal date
Ag-699.9**	2505	22.4	0.97	0.15	1.39 \pm 0.02	0.22 \pm 0.01	6.025	26 119 \pm 816
Ag-481.1	4196	20.7	0.73	0.42	1.34 \pm 0.01	0.45 \pm 0.01	3.289	63 903 \pm 1821
Ag-620.2**	6197	18	1.05	0.07	1.29 \pm 0.01	0.40 \pm 0.01	24.849	54 779 \pm 1778
Ag-481.2	4396	19	1.07	0.2	1.35 \pm 0.01	0.41 \pm 0.01	9.386	56 473 \pm 1302
Ag-481.3	4296	17.6	0.88	0.21	1.32 \pm 0.01	0.46 \pm 0.01	7.846	64 276 \pm 1852
Ag-620.5**	5997	16.7	1.08	0.12	1.32 \pm 0.01	0.48 \pm 0.01	17.876	68 954 \pm 1719
Ag-620.4	6097	15.5	1.37	0.26	1.28 \pm 0.01	0.48 \pm 0.01	9.898	69 012 \pm 2304
Ag-481.4	4496	16.4	0.96	0.3	1.28 \pm 0.01	0.53 \pm 0.01	6.637	78 572 \pm 2073
Ag-620.9**	5897	15.3	1.02	0.15	1.32 \pm 0.01	0.50 \pm 0.01	14.11	71 896 \pm 1768
Ag-699.7**	2805	14	1.1	0.15	1.28 \pm 0.01	0.59 \pm 0.01	17.828	92 094 \pm 3437
Ag-620.10b	6397	13.7	1.01	0.3	1.33 \pm 0.02	0.57 \pm 0.02	7.903	88 730 \pm 3954
Ag-620.10a	6297	13.7	0.89	0.34	1.28 \pm 0.02	0.59 \pm 0.02	6.113	94 007 \pm 4565
Ag-481.10**	6697	12.1	2.3	0	1.29 \pm 0.02	0.78 \pm 0.02	>100	148 302 \pm 8286
Ag-481.8**	1597	11.5	0.28	0.03	1.52 \pm 0.02	0.84 \pm 0.02	41.009	167 499 \pm 6824
Ag-481.9**	1697	10.9	0.82	0.1	1.48 \pm 0.02	0.84 \pm 0.02	33.104	169 285 \pm 8921
Ag-699.6**	3005	[7.9]***	1.19	0.12	1.63 \pm 0.02	1.62 \pm 0.04	82.663	>350 000

* Data from 3 key sections (AG-481, AG-620 and AG-699). Data in stratigraphical order.

** Data used for the Aguas river chronostratigraphy.

*** Travertine block is not in situ.

However, in contrast to the age overestimation which would be expected from this observation, all ages, except sample Ag-620.24, underestimate the expected age range defined by U/Th dating. Underestimated ages may be caused by anomalous fading of the feldspar luminescence signal although this could not be clarified

at this stage of the study. Preliminary fading tests (e.g. Auclair et al., 2003; Lamothe et al., 2003) have not yet yielded conclusive evidence for substantial fading. The most likely reason for the observed age underestimation could be a disequilibrium in the Uranium decay chain. At this site post-sedimentary enrichments of iron oxide

Table 2
Optical luminescence dating of fluvial deposits from the Alfaix sequence (Ag-620) and river terrace T4a (Ag-344)

Lab.-code	Sample	Uranium (ppm)	Thorium (ppm)	Potassium (%)		D_0 (Gy ka $^{-1}$) ^a	D_e (Gy) ^b	RSD (%)	n	Luminescence age (ka)
C-L1359	Ag-344.23	0.56 \pm 0.14	3.24 \pm 0.16	0.87 \pm 0.05	Q	1.24 \pm 0.08	35.4 \pm 1.9	33	37 (40)	< 29 (\pm 2)
					F	1.79 \pm 0.22	113 \pm 6	29	8 (11)	< 63 (\pm 8)
C-L1360	Ag-344.24	0.40 \pm 0.20	3.44 \pm 0.17	0.86 \pm 0.05	Q	1.21 \pm 0.09	26.2 \pm 1.4	54	34 (40)	< 22 (\pm 2)
					F	1.76 \pm 0.22	99 \pm 5	23	7 (11)	< 56 (\pm 8)
C-L1361	Ag-344.25	0.40 \pm 0.20	3.39 \pm 0.17	0.70 \pm 0.06	Q	1.06 \pm 0.10	40.2 \pm 2.1	38	37 (40)	< 38 (\pm 4)
					F	1.61 \pm 0.23	83 \pm 4	20	8 (12)	< 52 (\pm 8)
C-L1362	Ag-620.21	3.06 \pm 0.15	6.28 \pm 0.31	1.09 \pm 0.05	F	2.78 \pm 0.19	204 \pm 10	10	12 (13)	74 \pm 6
C-L1363	Ag-620.22	3.40 \pm 0.17	5.78 \pm 0.29	0.96 \pm 0.05	F	2.71 \pm 0.19	181 \pm 9	18	7 (7)	< 67 (\pm 6)
C-L1364	Ag-620.23	2.61 \pm 0.13	5.30 \pm 0.27	0.92 \pm 0.05	F	2.44 \pm 0.19	209 \pm 11	20	18 (19)	< 86 (\pm 8)
C-L1365	Ag-620.24	2.28 \pm 0.11	5.14 \pm 0.26	0.92 \pm 0.05	F	2.35 \pm 0.19	259 \pm 13	15	7 (7)	110 \pm 11

Radionuclide concentrations as measured by neutron activation analysis (NAA), calculated dose rates (D_0)^a for potassium-rich feldspars (F) and quartz (Q) and results of the equivalent dose (D_e) estimations derived from single aliquot regenerative-dose (SAR) measurements^b. RSD is the relative standard deviation of the $n D_e$ values used finally for D_e determination, which are statistically concordant with a normal distribution regarding the 5% significance level; the number of all measured aliquots is shown in parenthesis. Each D_e value represents the error weighted mean with the error including the standard error and a 5% uncertainty in the beta source calibration. All uncertainties, in the equivalent dose, dose rate and age determinations, represent the 1σ confidence interval.

^a The dose rate was calculated taking variations in the water content of 2 to 16 wt.% into account. For K-feldspars an internal potassium content of 12.5 \pm 0.5% (Huntley and Baril, 1997) and an alpha-efficiency factor of 0.07 \pm 0.02 (Preusser et al., 2005) was assumed.

^b Luminescence measurement parameters: a) BLSL (blue light stimulated luminescence) of quartz: pre-heat regeneration cycle 10 s at 240 °C, cut-heat test dose cycle TL 160 °C at 5 °C/s, stimulation 50 s BLSL at 125 °C, signal detection in the UV, aliquot size \sim 200 grains per sub-sample. b) IRSL (infrared stimulated luminescence) of K-feldspars: pre-heat regeneration and test dose cycle 10 s at 270 °C, stimulation 350 s IRSL at 50 °C, signal detection in the blue-violet (\sim 410 nm) wavelength range, aliquot size \sim 200 grains per sub-sample.

could have caused a Uranium excess. If so, then the U content measured by NAA overestimates the initial U content resulting in overestimated dose rates and finally in age underestimation. To verify these assumptions gamma spectrometry measurements still have to be carried out.

4.1.3. AMS

The AMS dating undertaken on two charcoal samples of terrace T4a overbank deposits provide calibrated ages of 5469–5309 cal BP (2 sigma, ID. Ua-24027) and 4085–3930 cal BP (2 sigma, ID. Ua-23276). The calibration was calculated using the Calib 5.0.2 programme.

4.2. Sedimentary environments of the key sections

A staircase of one pediment, 14 river depositional terraces and 4 Holocene valley fill terraces range in age from the upper Pliocene to the Holocene (Schulte, 2002a). Fig. 2 shows the longitudinal section of the middle reach of the River Aguas where 10 terraces are preserved.

In this paper the sediment records of specific key sections are considered: the +30 m terrace (G3), +13 m terrace (T3) and the Alfaix travertine sequence, located in the Aguas valley as it narrows between the villages of Alfaix and Turre (Fig. 2), plus the +8 m terrace (T4a) of the Rambla de los Hornos, a northern tributary of the lower River Aguas reach (Fig. 1).

In the middle Aguas valley, 2 km east of the Alfaix village, the +30 m fluvial terrace (G3; Fig. 2; site referred to as n° 1 in Fig. 1) is formed by a 2.5 m thick river channel deposit cemented at its base by iron oxides. On this polygenic gravel deposit fossil Bt and Bk soil horizons (haploxeralfs) are developed. The palaeosol is buried by a bioconstructed travertine representing the top of the sequence. The soil properties of a key profile of this terrace level near the village of Turre were published by Schulte and Julià (2001).

The next lower fluvial terrace T3 crops out at +13 m and is buried by a 10 m-thick travertine sequence (Figs. 3 and 4a; site referred to as n° 1 in Fig. 1). The lower unit of the terrace contains polygenic imbricated cobbles and pebbles in a sandy matrix (Fig. 4b) and also tilted and dislocated massive travertine blocks dated by U/Th as older than 350 kyr (the U/Th dating limit; Fig. 3; Table 1). The middle unit is formed by cross-bedded sands, layers of small-size local subangular quartzite and limestone pebbles and organic rich silt layers with frequent charcoal, gastropods and less abundant plant remains and oysters. Slope sediments dominate the lithology of the upper unit of the fluvial terrace (Fig. 4c). At the western edge of the key section the fluvial terrace

T3 overlies an older travertine platform formed by tilted and in situ massive travertine. U/Th dating of laminated travertine layers provides ages of 169 kyr and 148 kyr respectively (Fig. 4e).

The 10-m thick travertines overlying the +13 m terrace show progradational sloping surfaces interfingering with slope deposits (Fig. 4a). The bioconstructed travertines show different lithologies ranging from encrusted plant remains, algae and cyanobacterial lamination to bioclast accumulation (Fig. 4d). In the study area, the bioconstruction of travertine results from paludal environments so that the height of the ancient River Aguas bed can be inferred from the elevation of the Alfaix travertines. The fine grained slope deposits contain abundant angular local debris and some reworked fluvial gravels from terrace G3. Major paraconformities suggest the occurrence of various phases of travertine formation interrupted by incision events (Figs. 3 and 4a), whereas minor paraconformities of the upper platform are attributed to large scale cross-bedded travertine accretion caused by a westwards migration of the Aguas channel. Organic and calcic soil horizons (A and Bk horizons) developed on temporarily stable land-surfaces. The middle and upper units of the travertine sequence provide U/Th dates ranging from 92 to 26 kyr (Table 1 and Fig. 3).

Tectonics affected the travertine platforms in different ways. The lower platform shows complex tilting exceeding 10° (Fig. 4e), whereas the middle and upper platform are gently tilted <10° (Fig. 4f). Moreover, the north-western rim of the travertine platform including the +13 m terrace experienced subsidence.

The +8 m terrace T4a exposure at the Rambla de los Hornos consists of 3 m thick horizontal- and cross-bedded gravel channel deposits (Fig. 5; site referred to as n° 2 in Fig. 1). At the contact between the underlying Miocene marls and the base of the river terrace, carbonate precipitation occurred forming a thin calcic horizon and thin caps underneath the pebbles. OSL dating of the basal river channel deposits provides maximum ages of 28, 20 and 18 kyr. From the next younger terrace, the T4b terrace, located +6 m above the Rambla de los Hornos river bed, no ages were obtained. However, the T4a terrace deposition post-dates the incision that stopped the travertine formation of the Alfaix key section, dated by a maximum age of 26 kyr.

The gravel terrace T4a is buried by alluvial and colluvial deposits which display fossil organic soils (Cumulic Haploxerolls) dated from 5469–5309 and 4085–3930 cal. yrs B.P. (Fig. 5). Below the 3A horizon calcium carbonate nodules precipitated. Organic carbon reaches maximum values of 1.8% in the buried 2A

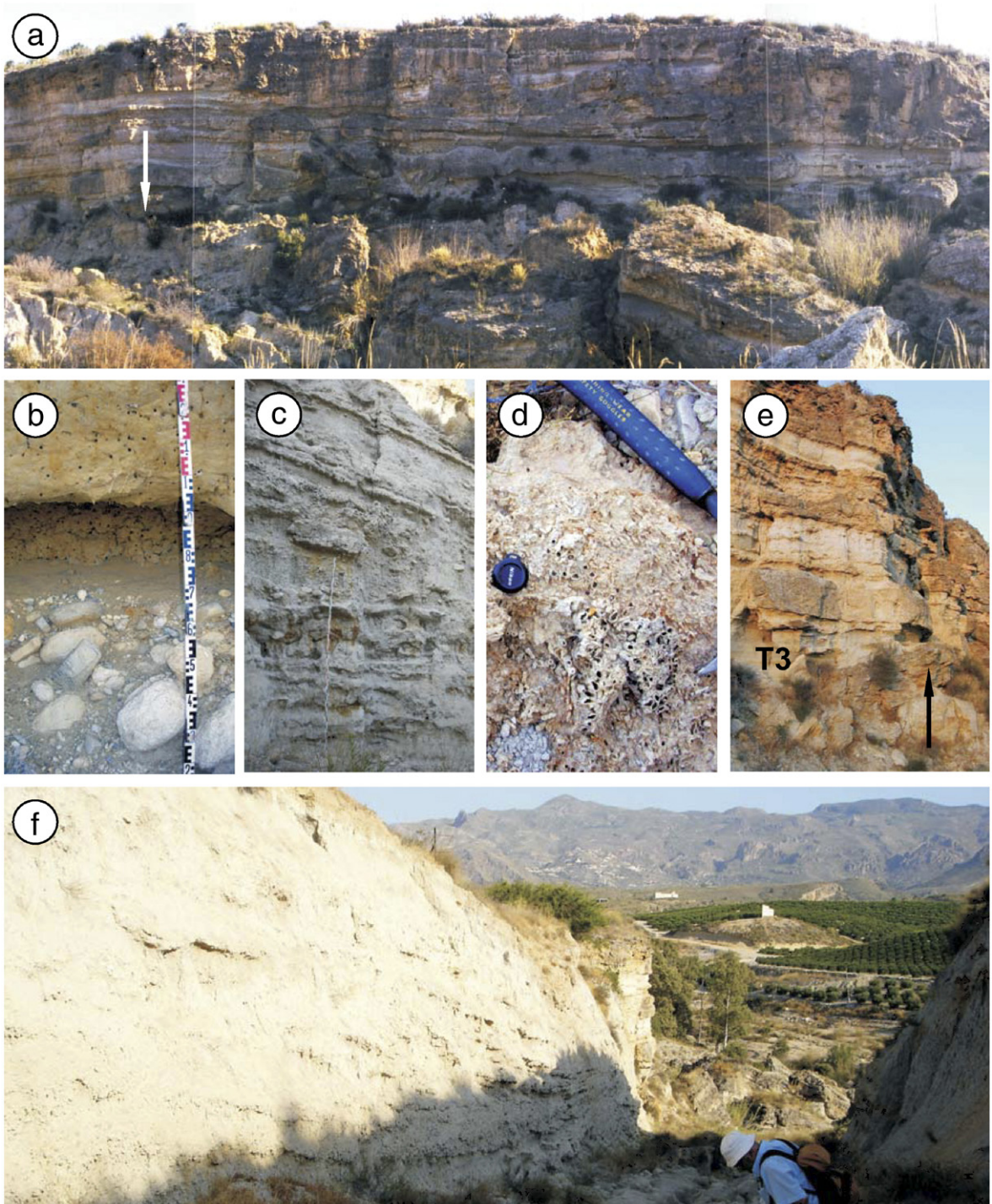


Fig. 4. Alfaix key section: 4a.—Travertine platform covering the T3 terrace. Note the paraconformities and the lateral accretion (from right to left) in upper unit. 4b.—Polygenic imbricated cobbles and pebbles in a sandy matrix from T3 terrace covered by the sands of the middle unit. 4c.—Slope deposits with travertine and reworked fluvial gravels covering silty beds. 4d.—Bioconstructed travertines showing incrustated plant remains. 4e.—View of the travertine platform as indicated by the white arrow in 4a showing travertine beds and detrital slope deposits. In the lower part, the fluvial sands of terrace T3 overly an older travertine platform formed by tilted massive travertine (black arrow). 4f.—Gently tilted slope deposits formed by silty sands and bioclast accumulation interfingering in the distal part not tilted travertine deposits. This view corresponds to the left part of the 4a.

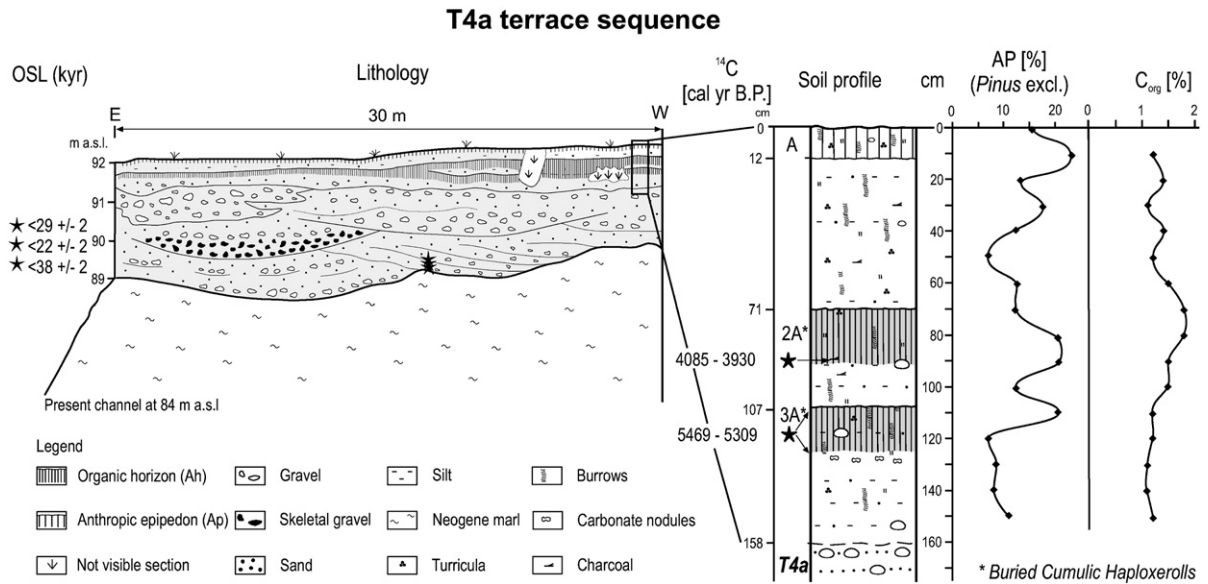


Fig. 5. Lithology of the fluvial terrace T4a key section. Geographical location in Fig. 1. Soil profile, arboreal pollen data and C_{org} are shown. Samples for OSL and radiocarbon dating are indicated in the fluvial terrace T4a and in the soil profile.

horizon. The most remarkable pedofeatures of this profile are the abundant worm casts with diameters of up to 1.7 cm and frequent turrlicula.

4.3. Palynological data of the key sections

4.3.1. The Pleistocene Alfaix travertine

The palynological record of the Alfaix travertines documents the continental palaeoenvironmental changes that occurred in the River Aguas catchment during the Upper Pleistocene (Fig. 6). The vegetation changes record both local (e.g. riparian and aquatic vegetation) and regional flora changes. Despite the low resolution of this sequence, two climatic conclusions can be reached:

1. The pollen spectra exhibit the permanent dominance of herbs suggesting that the climate of this area was unfavourable for the establishment of a forest, probably due to lengthy dry conditions.
2. On the basis of the pollen percentages of the regional vegetation (trees and herbs) and the pollen concentration, five pollen zones can be differentiated (Fig. 6):
 - a) The lower (zone A1a) is characterized by low pollen concentrations and arboreal pollen percentages. In this zone steppic taxa (*Artemisia*, *Chenopodiaceae*, *Ephedra*, *Lygeum*, *Asteraceae*) and general shrubs dominate suggesting dry climate conditions.
 - b) Zone A1b is also characterized by low arboreal pollen percentages and an increase in Poaceae percentages. In this zone *Pseudoschizaea* reach high

concentrations suggesting soil erosion (Pantaleón-Cano et al., 1996) probably due to the occurrence of more stormy rains.

c) Zone A2 is characterized by the rise of the thermophilous *Olea* and *Quercus* trees and the presence of deciduous oaks. These facts suggest a slight increase in regional humidity although the steppic and saline taxa such as *Artemisia*, *Chenopodiaceae*, *Cerealia*-type, and *Lygeum* support prevailing dry climate conditions.

d) Zone B1 is characterized by low arboreal pollen percentages and the expansion of shrub vegetation. The pollen spectra suggest a maquia landscape with steppic grassland patches.

e) Zone B2 is characterized by low arboreal and shrub pollen percentages and the presence of deciduous oaks. Despite these low values and the increase in *Artemisia* (characteristic of OIS 2, Burjachs and Allue, 2003) a certain increase in humidity is observed with respect to the previous zone. Nevertheless, dry conditions were dominant.

4.3.2. The Holocene alluvial deposits of the T4a terrace

The pollen analysis carried out on the 1.50 m Ag-443 key section records the environmental changes of the last 5500 yr cal. BP. The pollen diagram (Fig. 7) was established by 16 regularly spaced samples. The main characteristic of the entire pollen spectrum is the low value of arboreal pollen percentages (14.1–39.6% of AP) suggesting that during the Holocene regional climatic conditions were also unfavourable for forest

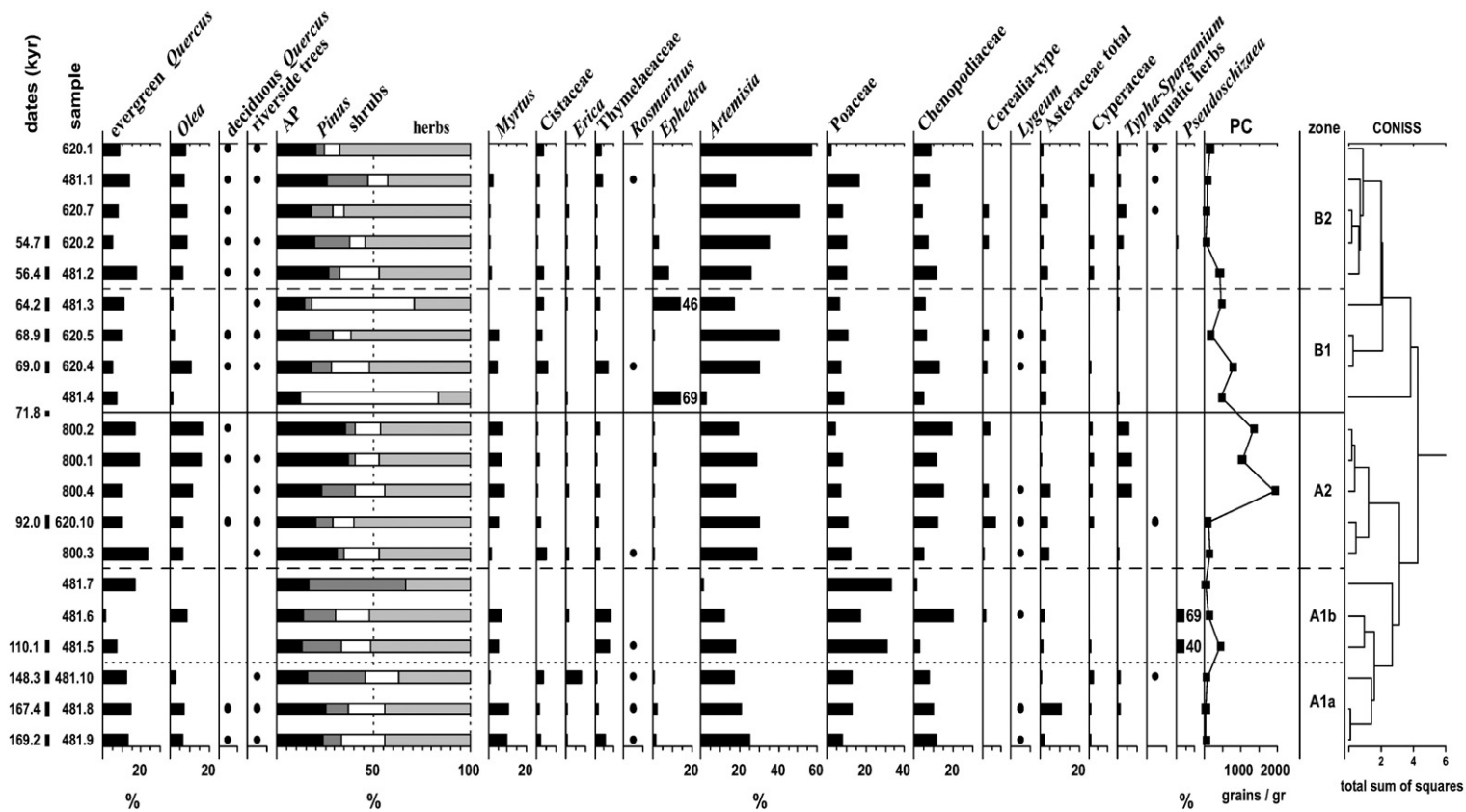


Fig. 6. Pollen diagram of the Aguas travertine key section. Dots indicate the presence of taxa lower than 5%. For sedimentary context and depth of the samples see Fig. 3.

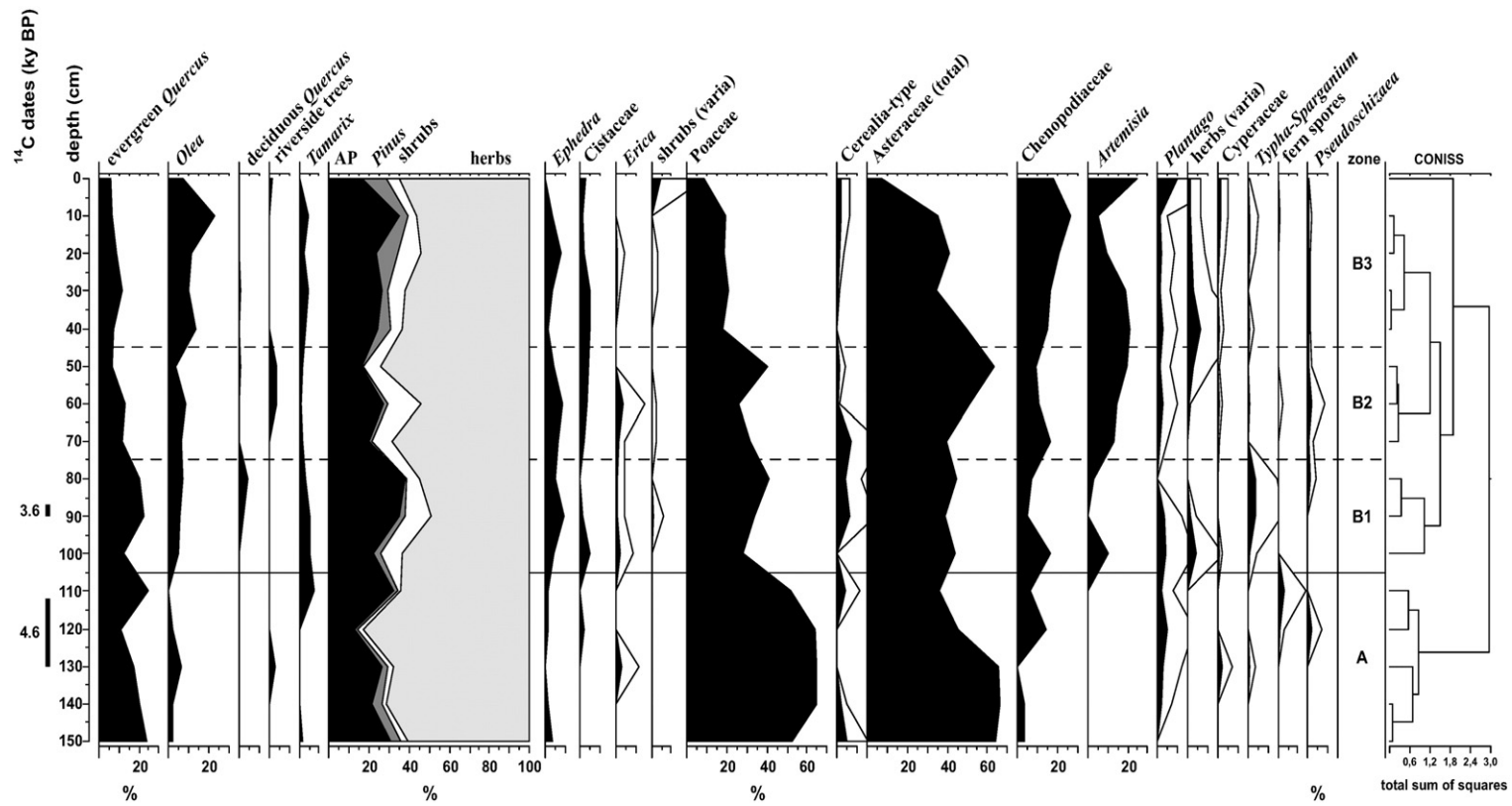


Fig. 7. Pollen diagram of the alluvial deposits of the T4a terrace.

development, as has been reported in the nearby Cabo de Gata sequence (Burjachs et al., 1997).

The lowest pollen zone (zone A, Fig. 7) records low AP percentages (14.1–35.6%) with *Quercus* evergreen, *Pinus* and *Olea* (wild olive tree). In wetland or riverside areas *Tamarix*, *Salix*, Cyperaceae herbs and *Typha–Sparganium* occurred. At the end of this zone, and conjoining with the mollic soil horizon, evergreen *Quercus* and *Tamarix* expanded. *Ephedra*, Cistaceae, and *Erica* were the main shrub taxa. The herb spectra show a steppic landscape of Asteraceae and wild Poaceae influenced by crops.

Zone B1 (Fig. 7) is characterized by an increase in AP percentages (25.6–38.8%). *Olea* increases its percentages and the pollen of the mesic deciduous *Quercus* records its highest percentages. The shrub vegetation formed by *Ephedra*, *Erica*, Cistaceae and *Rhamnus* also expanded at this time. The steppic herbs *Artemisia* and Chenopodiaceae show reduced pollen values at the same times that Cerealia and hygrophytes *Typha–Sparganium* values increased. This zone corresponds to a climate optimum and records the major taxonomic diversity of the pollen diagram. In addition, the mesic and hygrophyte taxa, as well as the increase in Cerealia, suggest moister climate conditions.

Zone B2 records a reduction of AP (29.0–17.2%) due to low percentages of *Quercus*, *Pinus* and *Tamarix*. Shrub vegetation shows higher diversity due to the presence of *Ephedra*, an increase of Cistaceae, *Erica*, Thymelaeaceae and *Periploca*, a relict taxa for the southeast of the Iberian Peninsula. The steppic taxa such as Asteraceae and *Artemisia* increase their percentages. All these facts suggest an increase in aridity.

The uppermost zone B3 is characterized by an increase in *Pinus* and *Olea*, which contributes to the AP rise (28.7–39.6%) and is probably a consequence of agricultural activities. The shrub taxa maintain their diversity with the presence of Cistaceae, *Ephedra*, *Erica* and Thymelaeaceae. The herbs are dominated by Asteraceae, *Artemisia* and *Plantago*, while Chenopodiaceae show a progressive increase. This increase in Chenopodiaceae is interpreted as a consequence of the expansion of the halophyte taxa due to the increase in aridity, although the pollen spectrum of the uppermost sample suggests a slight moisture increase.

5. Discussion

5.1. Chronostratigraphy of the River Aguas

The repeated cycles of downcutting, fluvial terrace deposition, and travertine plus colluvium aggradation suggest that the chronosequence of the River Aguas

provides a sensitive record of palaeoenvironmental changes. However, prior to 170 kyr, no precise radiometric dating were obtained, whereas from this point on, the chronological control improves substantially. The dynamics of the River Aguas and its possible correlation with regional and global palaeoclimate records are summarised in Fig. 8. The figure on the left shows the altitude of the past River Aguas bed, with respect to present day channel elevation, plotted versus age.

Regarding the Alfaix section several Pleistocene stratigraphical units were identified. The +30 m fluvial terrace G3 bears a haploxeralf palaeosol with Bt and Bk horizons, which was initially attributed to the upper Middle Pleistocene, according to the soil chronosequence provided by Schulte and Julià (2001). In the following discussion we return to the question of a more precise age estimation.

After the accumulation of the G3 terrace, major incision occurred, although at present it is not possible to define specific phases. The following chronostratigraphy starts with tilted travertine deposits dated to 169 kyr and in situ travertines dated to 148 kyr. Both units are separated by a paraconformity (Fig. 3). Following the sequence, a new phase of incision occurred prior to the deposition of the river terrace T3 that could be traced upstream to the upper Aguas reaching the Sorbas village (Schulte, 2002a). The T3 terrace contains at the Alfaix key section several tilted blocks, one of them dated by U/Th to older than 350 kyr (the U/Th dating limit; Fig. 3). These travertine blocks are remnants of prior travertine platforms that aggraded in the Alfaix area upstream of the Molino de la Cueva gorge (Fig. 2), perhaps predating even the +30 m terrace G3.

OSL dating of a sand layer from the fluvial terrace T3 at the Alfaix section provided ages of about 110, <86, 74 and <67 kyr (Fig. 3). However, all ages, except sample Ag-620.24 (Table 2), underestimate the expected age range obtained by U/Th dating (Table 1).

At least two significant incision events interrupted the aggradation of middle and upper units of the Alfaix travertine: the first occurred prior to 92 kyr (sample Ag-699.7 in Table 1) and the second at 71 kyr.

Palynological studies of 20 selected travertine samples covering the entire sequence indicate permanent dry environments (low values of AP and xeric taxa predominant, Fig. 5). Nevertheless, during the last episode of OIS 5 *Olea* and evergreen *Quercus* show maxima percentages suggesting moister conditions (Fig. 5; pollen zone A2). This assumption is supported by the presence of deciduous *Quercus* and riverside trees and the expansion of *Typha–Sparganium*. The travertine

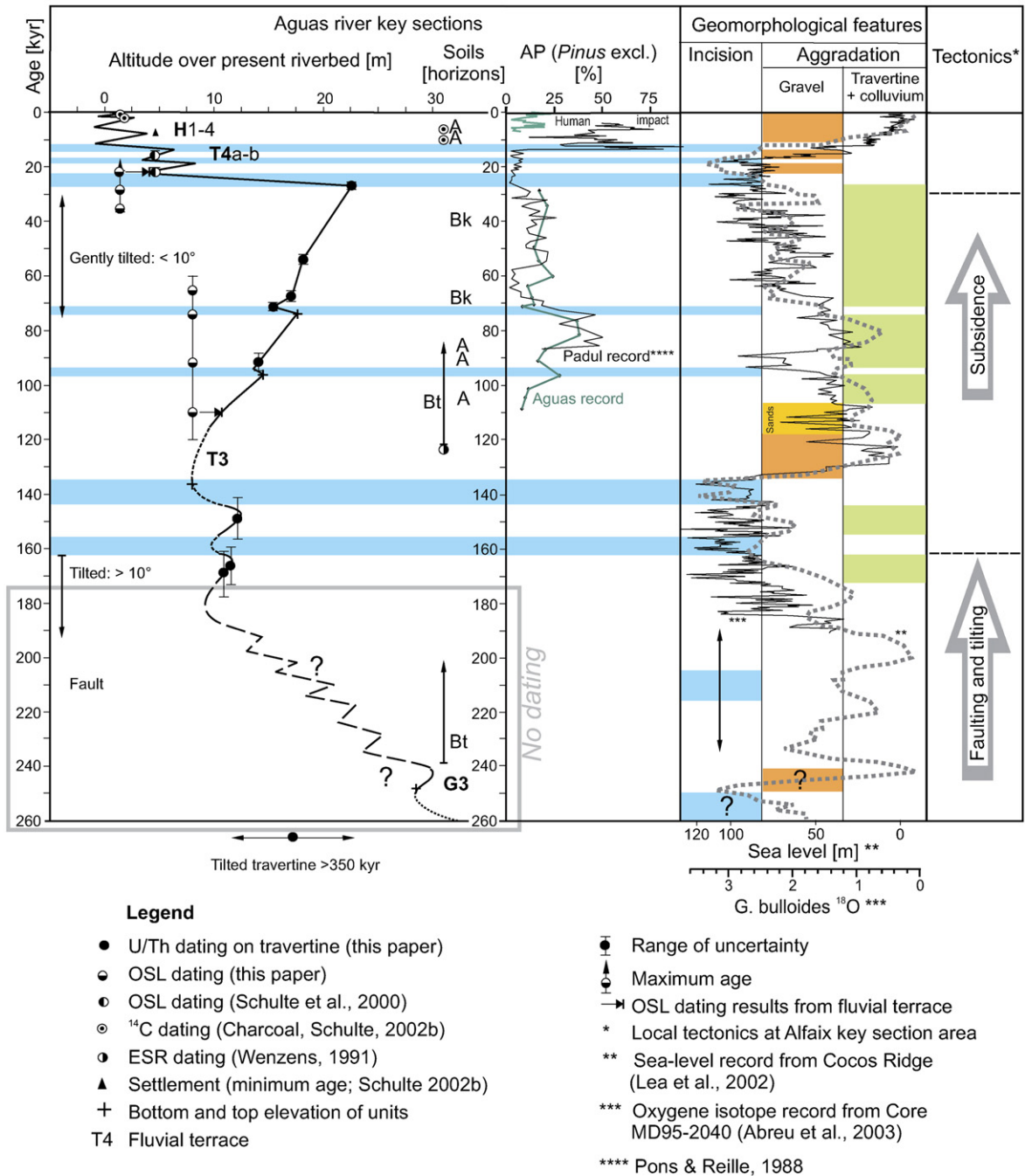


Fig. 8. Correlations between the River Aguas sequences and regional and global proxies.

sequence exhibits an incision event at 71 kyr, which corresponds to a reduction of arboreal pollen taxa.

The aggradation system collapsed after 26 kyr and steep downcutting occurred during OIS 2. Subsequently, basal river channel gravels of the +8 m terrace were deposited. Using the approach developed by Fuchs and

Lang (2001) for processing OSL data sets with a large scatter in equivalent dose values, ages of around 28, 20 and 18 kyr are obtained. According to the results of Schulte et al. (2000) in the Rambla Ancha (the site referred to as n° 3 in Fig. 1), a southern tributary of the lower River Aguas, one section shows four lower terraces

(T_I to T_{IV}) located between +8 m and +4 m above the river bed. Pedogenesis on these terraces is limited to the formation of haploxerolls. IRSL dating provided an age of 21.5 kyr for the oldest terrace T_I (+8 m) and 16.7 kyr (+5 m) for the third lower terrace T_{III} . These dates support the River Aguas chronostratigraphy.

The Holocene of the River Aguas is defined by five terraces, which developed, except for the higher one, during historical times between +4 and +2 m above river bed (Schulte, 2002b). Despite human influence during the Holocene, the increase in arboreal pollen taxa and the expansion of mesic pollen taxa confirm more humid climate conditions during the early and middle Holocene. The development of organic rich soils (haploxerolls), radiocarbon dated at 4.6 kyr BP and 3.6 kyr BP, confirms these climatic conditions.

5.2. Regional correlation

The northern portion of the Gibraltar Arc shows high diversity of fault slip rates (Negredo et al., 2002) causing an inhomogeneous tecto-sedimentary response. Various authors have tried to correlate different geomorphological units, such as palaeosols and river terraces (Völk, 1979; Günster et al., 2001). Until now their results have not been supported with accurate radiometric dates. In addition, the dated Middle and Late Quaternary river chronosequences of the Iberian Peninsula are located in different structural and climatic contexts (e.g. the Gallego and Cinca rivers in the Pyrenees studied by Sancho et al., 2004, the River Guadalope and the River Henares in the Iberian Range by Fuller et al., 1998 and Benito et al., 1998, the River Llobregat in the Catalan Ranges by Luque and Julià, 2007). In the Iberian Peninsula, the dated Late Pleistocene fluvial terraces show an inhomogeneous pattern with differences in the number of terrace levels or in their chronology (Santesteban and Schulte, in press). Thus, according to OSL dates, the three terrace levels differentiated in the Cinca and Gallego rivers (Qt6, Qt7, Qt8; Sancho et al., 2004) correlate with only one terrace (T7; Fuller et al., 1998) in the Guadalope river. These data do not support the hypothesis of synchronicity in major river aggradation events in Mediterranean catchments proposed by Macklin et al. (2002).

In the case of the River Aguas our chronostratigraphic model differs from those proposed by Kelly et al. (2000) and Candy et al. (2005) with respect to both the number of fluvial terraces and their chronology. The Kelly et al. (2000) and Candy et al. (2005) models were based on the terrace designation proposed by Harvey et al. (1995) and Harvey (2001), and the calcrete chronology of the upper reach of the River Aguas. This

is especially relevant for the C terrace of Harvey et al. (1995) and Harvey (2001) that aggraded before the River Aguas piracy. According to our chronostratigraphic model this terrace (the HT terrace of Schulte, 2002a) and the later river piracy are older than terrace G3 (Fig. 2). Following our age model (Fig. 8), terrace G3 probably aggraded during the OIS 8 to OIS7 transition around 250 kyr. As this terrace contains Filabres gneiss boulders from the upper Aguas catchment the piracy would be older than this age.

Other southern Spain travertine deposits that are preserved on stepped hillside slopes in Neogene basins show marked differences with the lower River Aguas chronologic model and drainage evolution. For example, in the Baza basin the upper River Fardes shows that the main downcutting triggering the badlands development occurred between 115 and 50 kyr (Díaz-Hernández and Julià, 2006). In the Granada basin, the four travertine terraces that are stepped near Nivar over 100 m in elevation, and dated between 290 and 11 kyr, show that the main incision took place during the Holocene (Martín-Algarra et al., 2003). These apparent discrepancies have resulted from the regional tectonic diversity and river capture.

5.3. The influence of neotectonics

Cyclic mechanisms such as climate and eustatic sea-level changes and tectonics are generally considered as factors triggering fluvial aggradation or downcutting although the relationship between these mechanisms and the chronostratigraphic data are not clearly established (Harvey, 2002). The River Aguas catchment area is developed over the Eastern branch of the Spanish Gibraltar Arc, a structure that constitutes part of the Africa–Iberian plate boundary. This area is characterized by the occurrence of large strike-slip faults such as the Carboneras, Palomares, Huerca-Overa and Lorca faults as a consequence of the NNW–SSE shortening. The Palomares fault (Faulkner et al., 2003; Booth-Rea et al., 2004), a NNE–SSW senestral trending fault impresses its strike-slip over the Aguas drainage pattern (Mather, 2000; Booth-Rea et al., 2004). A general uplift of this area has been also reported as a consequence of this faulting and 0.16 m kyr^{-1} of dip slip has been determined (Mather, 2000). Accordingly, the River Aguas flowing in an area with a measured uplift rate of 1.4 mm yr^{-1} (Giménez et al., 2000), has been characterised, over Quaternary timescales, by downcutting, whereas the Upper Pleistocene aggradation processes at the Alfaix travertine platform can partly be interpreted as the result of local subsidence. Regarding the Alfaix sequence, located in a fault controlled corridor,

we suggest that despite the aggradation period from 130 to 26 kyr, the general trend of Pleistocene river dynamics is dominated by incision as shown by the terrace sequence shown in Fig. 2. Uplift, faulting and tilting triggered this incisional trend, whereas subsidence affected travertine and colluvial aggradation. However, the tectonic factor does not satisfactorily explain general cyclic fluvial aggradation phases in the River Aguas system.

5.4. *The influence of eustatic sea-level and climate changes*

The influence of base-level changes from sea-level oscillation is widely discussed as the driving force of river response (Schumm, 1993; Harvey et al., 1999; Blum and Törnqvist, 2000; Litchfield and Berryman, 2005). Before we discuss sea-level changes as a controlling factor, we should first focus on the morphological setting of the study area and then on the possible correlation between the records of our key sections and global sea-level and regional oxygen isotope curves.

The outstanding feature of the morphological setting of the lower Aguas reach is the small distance between the continental slope and the present coastline. The shelf is narrow and shows much higher gradient (2.3°) than the slope of the coastal Aguas valley (0.34°) and channel profile (0.26°). The distance between the coastline and the 1000 m isobath is only 10 km and the 100 m isobath is about 2.5 km east of the River Aguas mouth. Therefore, the river could accommodate a lower sea-level not only through increased channel sinuosity but also by incision (Schumm, 1993). This hypothesis is supported by the traces of shelf channels shown by the Physiographic Map of the Littoral of Andalucía (Vanne and Menanteau, 1985) and by a 3D block diagram of the littoral of the Vera basin published by Díaz del Río Español and Fernández Salas (2005).

The possible connection between fluvial and oxygen proxies is compiled by Fig. 8. At first sight, the close correlation between the periods of changes in the River Aguas and the Cocos ridge oxygen isotope record (Lea et al., 2002), as well as the oxygen isotope record from the Atlantic Iberian margin in core MD95-2040 (Abreu et al., 2003), suggest that incision and aggradation periods could correspond to sea-level changes. Fig. 8 shows that major sea-level falls of the Cocos ridge record, with changes of 50 to 70 m, could affect the dynamics of the River Aguas in different ways. Limited incision (<2.5 m) of the River Aguas at the Alfaix site correlate with sea-level falls from 175 to 160 kyr and from 80 to 70 kyr, whereas major river incisions of 5 m and 17.5 m (Fig. 8) occurred from 145 to 140 kyr and from 30 to 20 kyr. In contrast, periods of

gravel terrace aggradation correlate to major sea-level rise of ca. 120 m at the OIS 6/5 and the OIS 2/1 boundary (Lea et al., 2002).

According to this pattern of river response, the deposition of the +30 m terrace probably corresponds to the sea-level rise from OIS 8 to 7. If sea-level oscillation was one of the driving factors on river incision and aggradation we suggest that only the falls to the lowest absolute sea-levels during isotope stages OIS 6 and 2 generated threshold crossing in the River Aguas system and major incision rates.

However, this pattern of sea-level change and river response is less convincing for the two youngest incision events. River abandonment of the floodplain surface of terrace T4a and T4b and incision of the order of 4 m and 6 m occurred approximately between 18 and 16 kyr and during the Younger Dryas. Both periods of downcutting may correlate to peaks of increased $\delta^{18}\text{O}$ in core MD95-2040. However, the river incision of 6 m during the Younger Dryas corresponds to a minor sea-level fall. Dias et al. (2000) postulate a Younger Dryas regression of 20 m for the Portuguese shelf, whereas Lohne et al. (2004) determined a sea-level fall of 9 m at the western Norwegian Atlantic coast.

Hence the question arises as to what degree of sea-level change would be required to produce the vertical changes in river channels observed during OIS 2. In the Aguas valley the intersection between the modern floodplain and the floodplain surface from the last Glacial Maximum is located 4 km from the coastline. Therefore, the upstream extent of coastal onlap due to sea-level rise is relatively small and does not reach the T4a key section, 9 km from the coastline. Although the basin fill of the lower Aguas valley is formed by erodible Neogene marls, the unconformity between Pleistocene alluvial deposits and underlying Neogene marls could be traced by drillings (Hoffmann, 1988) at relatively shallow depths: -12 m at the Aguas mouth, -26 m at the Antas mouth and -30 m at the Almanzora mouth. In the case of the River Aguas the channel cuts through the less erodible metamorphic rocks of the basement, thus reducing the affect of sea-level changes on the Aguas valley slope. Furthermore, a sequence of 6 or 7 marine terraces of raised Pleistocene beaches (Goy and Zazo, 1986; Wenzens, 1991; Schulte, 2002a) indicates the uplift of this basement along the Palomares fault zone near the Aguas mouth.

From these data we infer that sea-level change amplitude is not the only decisive driving factor for river profile response as pointed out by Blum and Törnqvist (2000). These authors show for low- and steep-gradient large river systems that the extension of Late Glacial Maximum channels is limited. Moreover, the argument

of Leeder and Stewart (1996) stresses the implications of high rates of sediment supply, which can overcome base-level fall and result in progradation without significant incision. However, the preservation of Pleistocene palaeosols as rhodoxeralfs and haploxeralfs in the Vera basin on terrace surfaces (Schulte and Julià, 2001) suggests that the variability of sediment yield was triggered by fluvial erosion and mass movement on slopes of the basin and surrounding ranges.

The question of climate control over river dynamics may be considered with regard to the correlations proposed in Fig. 8. The incision events of the River Aguas around 72, 25 and 11 kyr occurred simultaneously with the decrease of the arboreal vegetation indicated by the pollen records at Padul (Pons and Reille, 1988) and Alfaix (this paper).

In southern Spain these drops of AP % and mesic tree pollen % prior to human impact are mainly related to the increase of arid climatic conditions (Figs. 3, 6 and 8)). This transition to more arid climate conditions may have decreased the sediment yield from upstream sources, over longer timescales (Bull, 1991; Schumm, 1993). For example, historical flood records reconstructed from documentary data show that in the Mediterranean littoral of the Iberian Peninsula torrential rainstorms with increased runoff were more frequent during drier climate episodes (Barriendos and Martín Vide, 1998). Such a possible combination of reduced sediment supply and increased sediment transport rates may have led to sediment bypass and incision on the River Aguas. Both factors, climate-induced incision together with tectonic uplift, may have resulted in the observed increasing upstream difference in river terrace elevations.

Among the three cyclic mechanisms we suggest that large scale tectonics controlled the general downcutting trend, whereas the main aggradation and incision phases occurred during periods of major sea-level changes. The different terrace levels of OIS 2 show the influence of climate on river incision at medium time scales. Thus, the three cyclic mechanisms play an important role in triggering fluvial aggradation and downcutting, but at different time scales.

Moreover, synergetic processes should be considered with respect to abrupt incision/aggradation events, such as those recorded at the Alfaix key section. For example, the 13 m-aggradation from 130 to 26 kyr or the 17.5 m-incision around 25 kyr when climatic, sea-level and probably the tectonic regime could have amplified these fluvial events.

Furthermore, short events, such as the Younger Dryas (only 1.0 kyr, Hajdas et al., 2004), produced several river terraces, which are well preserved due to

their relatively young age. Similar events probably occurred in previous times but they are not easy to identify in the morphological record of the T3 sequence. However, the Alfaix travertine sedimentary record shows different phases of alternating travertine formation and colluvium aggradation resulting from these climatic change events.

6. Concluding remarks

Our results suggest that the fluvial archives of the River Aguas provide sensitive resolution records of environmental changes during the last 170 kyr. We have outlined the importance of chronology in understanding the timing, mechanism and driving forces of river dynamics. The application of different dating methods, including U/Th, OSL and ^{14}C , is important in order to identify uncertainties and the limits of each method, and to calibrate the chronological framework.

From the chronostratigraphic data sets we have established a model of middle and late Pleistocene river response for littoral basins of the southern Iberian Peninsula. Nonetheless, for river systems influenced by tectonics, climate and sea-level changes it is difficult to assess the weight of each controlling factor. Regarding the three mechanisms of Pleistocene river dynamics in middle-size catchment areas of the littoral of southeastern Spain, our results support the hypothesis that large scale tectonics triggered the general downcutting trend, whereas the main aggradation and incision phases occurred during periods of major sea-level changes. At short-time scales the influence of climate variability, as documented by pollen records, plays a decisive role. Thus, the river responses to the three cyclic mechanisms operate at different time scales.

The available age constraints suggest that terrace deposition was related to major environmental changes from OIS 6 to OIS 5 (terrace T3) and from OIS 2 to OIS 1 (terraces T4 and T4b) although Holocene sea-level and climate changes also produced valley fills.

Acknowledgements

Geochemical analysis was carried out at the Serveis Científic-Tècnics and the Laboratory of Landscape Ecology, University of Barcelona.

References

- Abreu, L. de, Shackleton, N.J., Schönfeld, J., Hall, M., Chapman, M., 2003. Millennial-scale oceanic climate variability off the Western Iberian margin during the last two glacial periods. *Marine Geology* 196, 1–20.

- Auclair, M., Lamothe, M., Huot, S., 2003. Measurement of anomalous fading for feldspar IRSL using SAR. *Radiation Measurements* 37, 487–492.
- Barriendos, M., Martín Vide, J., 1998. Secular climatic oscillations as indicated by catastrophic floods in the Spanish Mediterranean coastal Area (14th–19th centuries). *Climatic Change* 38, 473–491.
- Benito, A., Pérez-González, A., Santonja, M., 1998. Terrazas rocosas, aluviales y travertínicas del valle alto del río Henares (Guadalajara, España). *Geogaceta* 24, 55–58.
- Bischoff, J.L., Fitzpatrick, J.A., 1991. U-series dating of impure carbonates: an isochron technique using total-sample dissolution. *Geochimica et Cosmochimica Acta* 55, 543–554.
- Bischoff, J.L., Julià, R., Mora, R., 1988. Uranium-series dating of the Mousterian occupation at Abric Romaní, Spain. *Nature* 332, 68–70.
- Bischoff, J.L., Ludwig, K., Garcia, J.F., Carbonell, E., Vaquero, M., Stafford Jr., T.W., Jull, A.J.T., 1994. Dating of the Basal Aurignacian Sandwich at Abric Romaní (Catalunya, Spain) by Radiocarbon and Uranium-Series. *Journal of Archaeological Science* 21, 541–551.
- Blum, M.D., Törnqvist, T.E., 2000. Fluvial responses to climate and sea-level change: a review and look forward. *Sedimentology* 47 (Supplement 1), 2–48.
- Booth-Rea, G., Azañón, J.M., García-Dueñas, V., 2004. Extensional tectonics in the northeastern Betics (SE Spain): case study of extension in a multilayered upper crust with contrasting rheologies. *Journal of Structural Geology* 26, 2039–2058.
- Braga, J.C., Martín, J.M., Quesada, C., 2003. Patterns and average rates of late Neogene–Recent uplift of the Betic Cordillera, SE Spain. *Geomorphology* 50, 3–26.
- Bull, W.B., 1991. *Geomorphic Responses to Climatic Change*. Oxford University Press, Oxford.
- Burjachs, F., Allue, E., 2003. Paleoclimatic evolution during the last glacial cycle at the NE of the Iberian Peninsula. In: Ruiz, M.B., Dorado, M., Valdeolmillos, A., Gil, M.J., Bardají, T., de Bustamante, I., Martínez, I. (Eds.), *Quaternary Climatic Changes and Environmental Crises in the Mediterranean Region*. Ministerio de Ciencia y Tecnología and INQUA, Alcalá de Henares, pp. 191–200.
- Burjachs, F., Giralt, S., Roca, J.R., Seret, G., Julià, R., 1997. Palinología holocénica y desertización en el Mediterráneo occidental. In: Ibáñez, J.J., Valero Garcés, B.L., Machado, C. (Eds.), *El paisaje mediterráneo a través del espacio y del tiempo*. Geofoma Ediciones, Logroño, pp. 379–394.
- Burjachs, F., López-Sáez, J.A., Iriarte, M.J., 2003. Metodología arqueopalinológica. In: Buxó, R., Piqué, R. (Eds.), *La recogida de muestras en arqueobotánica: objetivos y propuestas metodológicas*. Museu d'Arqueologia de Catalunya, Barcelona, pp. 11–18.
- Candy, I., Black, S., Sellwood, B.W., 2005. U-series isochron dating of immature and mature calcretes as a basis for constructing Quaternary landform chronologies for the Sorbas basin, southeast Spain. *Quaternary Research* 64, 100–111.
- Dias, J.M.A., Boski, T., Rodrigues, A., Magalhães, F., 2000. Coast line evolution in Portugal since the Last Glacial Maximum until present — a synthesis. *Marine Geology* 170, 177–186.
- Díaz del Río Español, V., Fernández Salas, L.M., 2005. El margen continental del levante español y las Islas Baleares. In: Martín Serrano, A. (Ed.), *Mapa Geomorfológico de España y del margen continental a escala 1:1,000,000*. Instituto Geológico y Minero de España, Madrid, pp. 177–188.
- Díaz-Hernández, J.L., Julià, R., 2006. Geochronological position of badlands and geomorphological patterns in the Guadix–Baza basin (SE Spain). *Quaternary Research* 65, 467–477.
- Faulkner, D.R., Lewis, A.C., Rutter, E.H., 2003. On the internal structure and mechanics of large strike-slip fault zones: field observations of the Carboneras fault in southeastern Spain. *Tectonophysics* 367, 235–251.
- Florschütz, F., Menendez Amor, J., Wijnstra, T.A., 1971. Palynology of a thick Quaternary succession in southern Spain. *Palaeogeography Palaeoclimatology Palaeoecology* 10, 233–264.
- Fuchs, M., Lang, A., 2001. OSL dating of coarse-grain fluvial quartz using single-aliquot protocols on sediments from the NE Peloponnese, Greece. *Quaternary Science Reviews* 20, 783–787.
- Fuller, I.C., Macklin, M.G., Lewin, J., Passmore, D.G., Wintle, A.G., 1998. River response to high-frequency climate oscillations in southern Europe over the past 200 k.y. *Geology* 26, 275–278.
- Giménez, J., Suriñach, E., Goula, X., 2000. Quantification of vertical movements in the eastern Betics (Spain) by comparing levelling data. *Tectonophysics* 317, 237–258.
- Godfrey-Smith, D.I., Huntley, D.J., Chen, W.-H., 1988. Optical dating studies of quartz and feldspar sediment extracts. *Quaternary Science Reviews* 7, 373–380.
- Goëury, Cl., de Beaulieu, J.L., 1979. À propos de la concentration du pollen à l'aide de la liqueur de Thoulet dans les sédiments minéraux. *Pollen et Spores* 21, 239–251.
- Goy, J.L., Zazo, C., 1986. Synthesis of the Quaternary in the Almería litoral neotectonic activity and its morphological features, western Betics, Spain. *Tectonophysics* 130, 259–270.
- Gràcia, E., Pallàs, R., Soto, J.I., Comas, M., Moreno, X., Masana, E., Santanach, P., Díez, S., García, M., Dañobeitia, J., HITS scientific party, 2006. Active faulting offshore SE Spain (Alboran Sea): implications for earthquake hazard assessment in the Southern Iberian Margin. *Earth and Planetary Science Letters* 241, 734–749.
- Grafenstein, R., von Zahn, R., Tiedemann, R., Murat, A., 1999. Planctonic $\delta^{18}\text{O}$ records at sites 976 and 977, Alboran Sea: stratigraphy, forcing, and paleoceanographic implications. In: Zahn, R., Comas, M.C., Klaus, A. (Eds.), *Proceedings of the Ocean Drilling Programme, Scientific Results*, vol. 161, pp. 469–479.
- Gregory, K.J., Benito, G., Dikau, R., Golosov, V., Johnston, E.C., Jones, J.A.A., Macklin, M.G., Parson, A.J., Passmore, D.G., Poesen, J., Soja, R., Starkel, L., Thorndycraft, V.R., Walling, D.E., 2006. Past hydrological events and global change. *Hydrological Processes* 20, 199–204.
- Günster, N., Eck, P., Skowronek, A., Zöller, L., 2001. Late Pleistocene loess and their paleosols in the Granada Basin, Southern Spain. *Quaternary International* 76/77, 241–245.
- Hajdas, I., Bonani, G., Hadorn, P., Thew, N., Coope, G.R., Lemdahl, G., 2004. Radiocarbon and absolute chronology of the Late-Glacial record from Hauterive/Rouges-Terres, Lake Neuchâtel (CH). *Nuclear Instruments and Methods in Physics Research Section B: Beam Interactions with Materials and Atoms*, vol. 223–224, pp. 308–312.
- Harvey, A.M., 2001. Uplift, dissection and landform evolution: the Quaternary. In: Mather, A.E., Martín, J.M., Harvey, A.M., Braga, J.C. (Eds.), *A field guide to the Neogene sedimentary basins of the Almería Province, South–East Spain*. Blackwell Science, London, pp. 225–322.
- Harvey, A.M., 2002. Effective timescales of coupling within fluvial systems. *Geomorphology* 44, 175–201.
- Harvey, A.M., Miller, S.Y., Wells, S.G., 1995. Quaternary soil and river terrace sequences in the Aguas/Feos river systems: Sorbas basin, southeast Spain. In: Lewin, J., Macklin, M.G., Woodward, J.C.

- (Eds.), *Mediterranean Quaternary River Environments*. Balkema, Rotterdam, pp. 263–281.
- Harvey, A.M., Silva, P.G., Mather, A.E., Goy, J.L., Stokes, M., Zazo, C., 1999. The impact of Quaternary sea-level and climatic change on coastal alluvial fans in the Cabo de Gata ranges, southeast Spain. *Geomorphology* 28, 1–22.
- Hoffmann, G., 1988. *Holozänstratigraphie und Küstenlinienverlagerung an der andalusischen Mittelmeerküste*. Berichte aus dem Fachbereich Geowissenschaften der Universität Bremen, Bremen 173.
- Huntley, D.J., Baril, M.R., 1997. The K content of K-feldspars being measured in optical and thermoluminescence dating. *Ancient TL* 15, 11–13.
- ICONA, 1991. Mapa de suelos, escala 1:100000, Vera — 1014. Proyecto Lucdeme. ICONA, Universidad de Granada, Granada.
- Ivanovich, M., Harmon, R.S. (Eds.), 1982. *Uranium Series Disequilibrium: Applications to Environmental Problems*. Clarendon Press, Oxford, p. 571.
- Julià, R., Bischoff, J.L., 1991. Radiometric dating of Quaternary deposits and of the Hominid mandible of lake Banyoles, Spain. *Journal of Archaeological Science* 18, 707–722.
- Kageyama, M., Combourieu Nebout, N., Sepulchre, P., Peyron, O., Krinner, G., Ramstein, G., Cazet, J.-P., 2005. The Last Glacial Maximum and Heinrich Event 1 in terms of climate and vegetation around the Alboran Sea: a preliminary model-data comparison. *Comptes Rendus Geosciences* 337, 983–992.
- Kelly, M., Black, S., Rowan, J.S., 2000. A calcrite-based U/Th chronology for landform evolution in the Sorbas basin, southeast Spain. *Quaternary Science Reviews* 19, 995–1010.
- Lamothe, M., Auclair, M., Hamzaoui, C., Huot, S., 2003. Towards a prediction of long-term anomalous fading of feldspar IRSL. *Radiation Measurements* 37, 493–498.
- Lea, D.W., Martin, P.A., Pak, D.K., Spero, H.J., 2002. Reconstructing a 350 ky history of sea level using planktonic Mg/Ca and oxygen isotope records from a Cocos Ridge core. *Quaternary Science Reviews* 21, 283–293.
- Leeder, M.R., Stewart, M.D., 1996. Fluvial incision and sequence stratigraphy: alluvial responses to relative sea-level fall and their detection in the geological record. *Geological Society Special Publication* 103, 25–39.
- Litchfield, N.J., Berryman, K.R., 2005. Correlation of fluvial terraces within the Hikurangi Margin, New Zealand: implications for climate and base-level controls. *Geomorphology* 68, 291–313.
- Lohne, Ø.S., Bondevik, S., Mangerud, J., Schrader, H., 2004. Calendar year age estimates of Allerød-Younger Dryas sea-level oscillations at Os, western Norway. *Journal of Quaternary Science* 19, 443–464.
- López Casado, C., Sanz de Galdeano, C., Molina Palacios, S., Henares Romero, J., 2001. The structure of the Alboran Sea: an interpretation from seismological and geological data. *Tectonophysics* 338, 79–95.
- Loublier, Y., 1978. Application de l'analyse pollinique à l'étude du paléoenvironnement du remplissage Würmien de la grotte de L'Arbreda (Espagne). *Académie de Montpellier (U.S.T.L.)*, Montpellier.
- Luque, J.A., Julià, R., 2007. U/Th dating of Quaternary travertines at the middle River Llobregat (NE Iberian Peninsula, Northwestern Mediterranean). Correlation with sea-level changes. *Geologica Acta* 5, 109–117.
- Macklin, M.G., Fuller, I.C., Lewin, J., Maas, G.S., Passmore, D.G., Rose, J., Woodward, J.C., Black, S., Hamlin, R.H.B., Rowan, J.S., 2002. Correlation of fluvial sequences in the Mediterranean basin over the last 200 ka and their relationship to climate change. *Quaternary Science Reviews* 21, 1633–1641.
- Martín-Algarra, A., Martín-Martín, M., Andreo, B., Julià, R., González-Gómez, C., 2003. Sedimentary patterns in perched spring travertines near Granada (Spain) as indicators of the paleohydrological and paleoclimatological evolution of a karst massif. *Sedimentary Geology* 161, 217–228.
- Mather, A.E., 2000. Adjustment of a drainage network to capture induced base-level change: an example from the Sorbas Basin, SE Spain. *Geomorphology* 34, 271–289.
- Mather, A.E., Harvey, A.M., Brenchley, P.J., 1991. Halokinetic deformation of Quaternary river terraces in the Sorbas Basin, southeast Spain. *Zeitschrift für Geomorphologie. N.F. Supplement-Bd.* 82, 87–97.
- Montenat, C., Ott d'Estevou, Ph., Rodríguez Fernandez, J., Sanz de Galdeano, C., 1990. Geodynamic evolution of the betic neogene intramontane basins (S and SE Spain). *Paleontologia i Evolució* 2, 7–16.
- Moreno, A., Cacho, I., Canals, M., Prins, M.A., Sánchez-Goñi, M.F., Grimalt, J.O., Weltje, G.J., 2002. Saharan dust transport and high-latitude glacial climatic variability: the Alboran Sea record. *Quaternary Research* 58, 318–328.
- Murray, A.S., Wintle, A.G., 2000. Luminescence dating of quartz using an improved single-aliquot regenerative-dose protocol. *Radiation Measurements* 32, 57–73.
- Negredo, A.M., Bird, P., Sanz de Galdeano, C., Buforn, E., 2002. Neotectonic modelling of the Ibero-Maghrebian region. *Journal of Geophysical Research* 107 (B11), 10.1–10.15.
- Pantaleón-Cano, J., Pérez-Obiol, R., Yll, E.I., Roure, J.M., 1996. Significado de Pseudoschizaea en las secuencias sedimentarias de la vertiente mediterránea de la Península Ibérica e Islas Baleares. In: Ruiz Zapata, B. (Ed.), *Estudios palinológicos*. Universidad de Alcalá. Alcalá de Henares, pp. 101–105.
- Preusser, F., Andersen, B.G., Denton, G.H., Schlüchter, C., 2005. Luminescence chronology of Late Pleistocene glacial deposits in North Westland, New Zealand. *Quaternary Science Reviews* 24, 2207–2227.
- Pons, A., Reille, M., 1988. The Holocene- and Upper Pleistocene record from Padul (Granada, Spain): a new study. *Palaeogeography, Palaeoclimatology, Palaeoecology* 66, 243–263.
- Rivas Martínez, S., 1987. Memoria del mapa de series de vegetación de España. Instituto para la Conservación de la Naturaleza (ICONA). Ministerio de Agricultura, Pesca y Alimentación, Madrid.
- Roep, Th. B., Dabrio, C.J., Fortuin, A.R., Polo, M.D., 1998. Late highstand patterns of shifting and stepping coastal barriers and washover-fans (late Messinian, Sorbas Basin, SE Spain). *Sedimentary Geology* 116, 27–56.
- Sancho, C., Peña, J.L., Lewis, C., McDonald, E., Rhodes, E., 2004. Registros fluviales y glaciares cuaternarios en las cuencas de los ríos Cinca y Gállego (Pirineos y depresión del Ebro). In: Colombo, F., Iesa, C.L., Meléndez, G., Pocoví, A., Sancho, C., Soria, A.R. (Eds.), *VI Congreso Geológico de España. Geo-Guías 1. Itinerarios Geológicos por Aragón*, pp. 181–205.
- Santisteban, J.I., Schulte, L., in press. Fluvial networks of the Iberian Peninsula: a chronological framework. *Quaternary Science Reviews*.
- Schulte, L., 1998. Quaternary morphodynamic and climate changes in the middle and lower Aguas Valley. In: Castro, P.V., Chapman, R.W., Gili, S., Lull, V., Micó, R., Rihuete, C., Risch, R., Sanahuja Yll, M.E. (Eds.), *Aguas Project. Paleoclimatic reconstruction and the dynamics of human settlement and land-use in the area of the middle Aguas*

- (Almería), in the south-east of the Iberian Peninsula. European Commission, D.G.XII, Brussels, pp. 35–39.
- Schulte, L., 2002a. Evolución cuaternaria de la depresión de Vera y de Sorbas oriental (SE-Península Ibérica): reconstrucción de las fluctuaciones paleoclimáticas a partir de estudios morfológicos y edafológicos. Publicaciones de la Universidad de Barcelona, Barcelona.
- Schulte, L., 2002b. Climatic and human influence on river systems and glacier fluctuations in southeast Spain. *Quaternary International* 93–94, 85–100.
- Schulte, L., 2003. River-response and terrace aggradation in the Mediterranean Iberian Peninsula during historical times. In: Thorndycraft, V.R., Benito, G., Barriendos, M., Llasat, M.C. (Eds.), *Palaeofloods, Historical Data and Climate Variability*. European Commission — CSIC, Madrid, pp. 67–72.
- Schulte, L., Julià, R., 2001. A Quaternary soil chronosequence of Southeastern Spain. *Zeitschrift für Geomorphologie* 45, 145–158.
- Schulte, L., Gómez Ortiz, A., Passmore, P., 2000. Sobre los supuestos restos periglaciares pleistocenos en los llanos del sureste de la Península Ibérica. In: Peña Monné, J.L., Sánchez-Fabre, M., Lozano, M.V. (Eds.), *Procesos y formas periglaciares en la montaña Mediterránea*. I.P.A.-España, Teruel, pp. 281–297.
- Schumm, S.A., 1993. River response to baselevel change: implications for sequence stratigraphy. *Journal of Geology* 101, 279–294.
- Stokes, M., Mather, A.E., 2003. Tectonic origin and evolution of a transverse drainage: the Río Almanzora, Betic Cordillera, Southeast Spain. *Geomorphology* 50, 59–81.
- Thorndycraft, V.R., Benito, G., 2006. The Holocene fluvial chronology of Spain: evidence from a newly compiled radiocarbon database. *Quaternary Science Reviews* 25, 223–234.
- Vandenberghe, J., 2003. Climate forcing of fluvial system development: an evolution of ideas. *Quaternary Science Reviews* 22, 2053–2060.
- Vanne, J.-R., Menanteau, L. (Eds.), 1985. *Mapa Fisiográfico del Litoral de Andalucía*. Junta de Andalucía, Sevilla.
- Völk, H., 1967. *Zur Geologie und Stratigraphie des Neogenbeckens von Vera, Südostspanien*. Univ. Amsterdam, Wageningen.
- Völk, H., 1979. Quartäre Reliefentwicklung in Südost-Spanien. *Heidelberger Geographische Arbeiten* 58 143 pp.
- Wallinga, J., 2001. The Rhine–Meuse system in a new light: optically stimulated luminescence dating and its application to fluvial deposits. *Netherlands Geographical Studies* 290 180 pp.
- Wallinga, J., Murray, A., Wintle, A., 2000. The single-aliquot regenerative-dose (SAR) protocol applied to coarse-grain feldspar. *Radiation Measurements* 32, 529–533.
- Wenzens, G., 1991. Die quartäre Küstenentwicklung im Mündungsberich der Flüsse Aguas, Antas und Almanzora in Südostspanien. *Erdkundliches Wissen* 105, 131–150.
- Wenzens, G., 1992. The influence of tectonics and climate on the Villafranchian Morphogenesis in semiarid Southwestern Spain. *Zeitschrift für Geomorphologie N.F. Supplement-Bd.* 84, 173–184.